# Novel Brush-Type Copolymers Bearing Thiophene Backbone and Side Chain Quinoline Blocks. Synthesis and Their Use as a Compatibilizer in Thiophene−Quinoline Polymer Blends

**Solon P. Economopoulos,[†,‡] Christos L. Chochos,[†,‡] Vasilis G. Gregoriou,[‡] Joannis K. Kallitsis,*[,†,‡] Sophie Barrau,[§] and Georges Hadziioannou[§]**

*Department of Chemistry, University of Patras, Patras, 26500, Greece, Foundation for Research and Technology-Hellas, Institute of Chemical Engineering and High Temperature Processes (FORTH−ICE/HT), Patras 26500, Greece, and Laboratoire d'Ingénierie des Polymères pour les Hautes Technologies, UMR 7165, Université Louis Pasteur, Ecole Européenne de Chimie, Polymères et Matériaux, 25, rue Becquerel, 67000 Strasbourg, France*

*Received September 5, 2006; Revised Manuscript Received December 7, 2006*

ABSTRACT: New copolymers bearing different degree of grafted polyquinoline segments onto a polythiophene backbone were obtained via atom transfer radical polymerization of a vinyl quinoline monomer using a properly modified polythiophene backbone as macroinitiator. The initiator preparation was based on the bromination to a certain extent of a commercially available poly(3-hexylthiophene-2,5-diyl) (P3HT) and subsequent conversion of the bromine groups to proper propionyl bromide units through a three-step process. Polymerization of the vinyl quinoline monomer, using typical ATRP conditions, resulted in the desired copolymers, which were effectively characterized using $^1$H NMR, UV−vis, and luminescence spectroscopy, as well as cyclic voltammetry. These copolymers were used in order to study their compatibilization efficiency in an immiscible P3HT/polyquinoline blend, which has been tested previously with respect to its photovoltaic efficiency. A detailed morphology study using atomic force microscopy (AFM) has shown that nanophase separated systems were obtained and the domain size was dependent on the blend composition, as well as the copolymer grafting density.

## Introduction

The realization that organic conjugated polymers can be used as electron donors and their combination to electron accepting phases can lead to efficient photovoltaic devices[1] has stimulated an intensive synthetic effort toward the development of new materials for organic photovoltaic applications. The bulk heterojunction architecture is particularly attractive due to its advantages in the combination of materials with donor and accepting properties.[2,3] This approach has proven very successful and has established its place as the most promising architecture for high performance polymer photovoltaics.

Among many different attempts, conjugated polymers have been combined with electron accepting phases, in order to form an extensive interface and also the appropriate morphology, resembling an interpenetrating network, providing the paths for hole and electron transport. Polymers such as MEH−PPV and P3HT have been the donor polymers of choice for polymer photovoltaics in the past decade, although recent attempts to maximize solar absorption have yielded interesting products.[4] As acceptor phases, soluble fullerene derivatives have given the best results so far, exhibiting 5% energy conversion efficiencies,[5] but there is also the tendency for the development of non-fullerenic electron accepting polymers.[6−10]

It was realized that the phase separation together with the proper selection of the donor and acceptor phases, plays a critical role in delivering a proper morphology.[11] Because of the certain advantages that copolymers possess, over polymer blends, to form well-defined and controlled morphologies, several groups have tried to combine the desired electron accepting and donating phases. Alternating or random copolymers obtained through polycondensation reactions have been synthesized.[12] In cases where fullerene derivatives were used as the accepting phase, controlled polymerization techniques have been employed.[13−17] Furthermore, recently, the copolymer approach with fullerene derivatives as the electron acceptors, yielded solar cell efficiencies near 2%.[18] Finally, compatibilization of P3OT/$C_{60}$ blends has been attempted by the use of a thiophene plasticizer.[19]

It is well-known that in polymer blends, copolymers are often used to compatibilize the immiscible pairs. This approach has yet to be tested in photovoltaic systems. The ability to synthesize copolymers having segments of the homopolymers used as the active layer, is the key factor. Thus, using a polymeric backbone which possesses a certain function (electron donating or accepting properties) and giving the ability to be modified and act as macroinitiator for the controlled radical polymerization of various vinylic monomers which possess the complementary function, will lead to the formation of a bifunctional copolymer which will effectively compatibilize the immiscible pair of the two homopolymers.

In this paper we wish to report on the synthesis of brush-type copolymers having a polythiophene backbone and polyquinolines as side groups, obtained by atom transfer radical polymerization of a vinyl quinoline monomer. A properly modified polythiophene was used as the macroinitiator. This copolymer has been used to study the compatibilizing efficiency in a poly(3-hexylthiophene-2,5-diyl)/polyquinoline system.

## Experimental Section

All solvents and reagents were supplied from Aldrich and were used without further purification unless otherwise stated.

* Corresponding author. E-mail address: j.kallitsis@chemistry.upatras.gr.
† Department of Chemistry, University of Patras.
‡ Foundation for Research and Technology-Hellas, Institute of Chemical Engineering and High Temperature Processes (FORTH−ICE/HT).
§ Laboratoire d'Ingénierie des Polymères pour les Hautes Technologies, UMR 7165, Université Louis Pasteur, Ecole Européenne de Chimie, Polymères et Matériaux.

10.1021/ma062055c CCC: $37.00 
Published on Web 01/27/2007

Bromo-P3HT (P3B4HT)[20] and the quinoline monomer (SDPQ)[21] were synthesized according to literature methods. *N*-Bromosuccinimide was recrystallized from water and stored under Ar before use. Diphenyl ether was purged with argon for 1 h before use. Triethylamine and dichloromethane were distilled and stored over molecular sieves prior to usage.

Optical absorption spectra were recorded on a Hewlett-Packard 8452A spectrophotometer. Photoluminescence spectra were recorded using a Perkin-Elmer LS45 luminescence spectrometer, by excitation of the sample at the absorption maxima of the UV−vis spectra. Polymeric films were fabricated either from spin-coating or drop casting of dilute solutions (0.2 mg, 10 mL).

$^1$H NMR spectra were obtained on a Bruker Avance-DPX 400 MHz with $CDCl_3$ having TMS as internal standard.

Cyclic voltammetry (CV) studies were performed using a standard three-electrode cell. Platinum wires were used as counter and working electrodes. Silver/silver nitrate (0.1 M $AgNO_3$ in acetonitrile) was used as a reference electrode. Tetrabutylammonium hexafluorophosphate ($(TBA)PF_6$) 98% from Aldrich was used as electrolyte and was recrystallized three times from acetone and was dried in vacuum at 100 °C before each experiment. Ferrocene was provided from Aldrich and was purified by sublimation before the experiments. Acetonitrile anhydrous 99.8%($CH_3CN$) was also supplied from Aldrich and was used without further purification. All experiments were carried out in an air-sealed electrochemical cell. Before each experiment, the cell was purged with high purity inert gas for 15 min. Before the start of the measurement the inert gas was turned to "blanket mode". Measurements were recorded using a EG&G Princeton Applied Research potensiostat/galvanostat model 263A connected to a personal computer running PowerSuite software. The working electrode was cleaned before each experiment through sonication in 65% $HNO_3$, followed by subsequent sonication in absolute EtOH. The $Ag/AgNO_3$ electrode was connected to the electrochemical cell through a salt bridge and was calibrated before each experiment by running cyclic voltammetry on ferrocene. The potential values obtained vs $Ag/Ag^+$ were converted vs saturated calomel electrode (SCE). The energy levels were calculated using the following empirical equation[22]

$$\mathrm{HOMO} = 4.4 + (E^{\mathrm{ox}}{}_{\mathrm{onset}}) \quad \text{and} \quad \mathrm{LUMO} = 4.4 + (E^{\mathrm{red}}{}_{\mathrm{onset}})$$

Samples were prepared by dipping the working electrode in a viscous 10 wt % chloroform solution of the polymers and subsequent drying.

Tapping mode atomic force microscopy (TM-AFM) images were performed with a Nanoscope IIIa microscope from Digital Instruments (operating in air, 25 °C). The microcantilever is a silicon tip with a force constant of 21−98 N/m and a resonance frequency of 146−236 kHz. The instrument provide simultaneously height and phase cartography. For AFM investigations, the samples were deposited by spin-coating of a solution (1 mg/mL of the copolymer in chloroform) onto mica substrates. Chloroform is a good solvent for the copolymer as well as the thiophene and quinoline homopolymers thus preventing aggregation in solution. The deposits were realized at 1500 rpm during 1 min followed by a rotational speed of 3000 rpm for a second minute. The films were then dried for 1−2 h under vacuum.

**Synthetic Procedure. Synthesis of 1ii.** In a round flask that was degassed, 220 mg (1,30mmol) of P3HT were dissolved in 20 mL of $CHCl_3$ under Ar atmosphere. The flask was covered with aluminum foil, and 120 mg (0.67mmol) of *N*-bromosuccinimide were added. The reaction was stirred at room temperature for 24 h. Then the mixture was heated at 50 °C. After 3 h, the heating was removed, 40 mL of distilled $H_2O$ was added, and the mixture was stirred at room temperature. The aqueous layer was extracted with $CH_2Cl_2$, and the organic layer was evaporated under reduced pressure. To the dried product was added ethanol, and the polymer was stirred 24 h and subsequently filtered and dried, yielding 250 mg of the partially substituted Br−P3HT (**1ii**).

$^1$H-NMR ($CDCl_3$): $\delta$ 7.05 (d, 1H), 2.81 (broad, 2H), 2.7 (broad, 2H), 1.56 (d, 4H), 1.28−1.33 (m, 12H), 0.91 (d, 6H).

**Scheme 1. Synthetic Procedure of Initiators 4i and 4ii and the Resulting Thiophene Quinoline Brush-Type Copolymers 5i and 5ii**

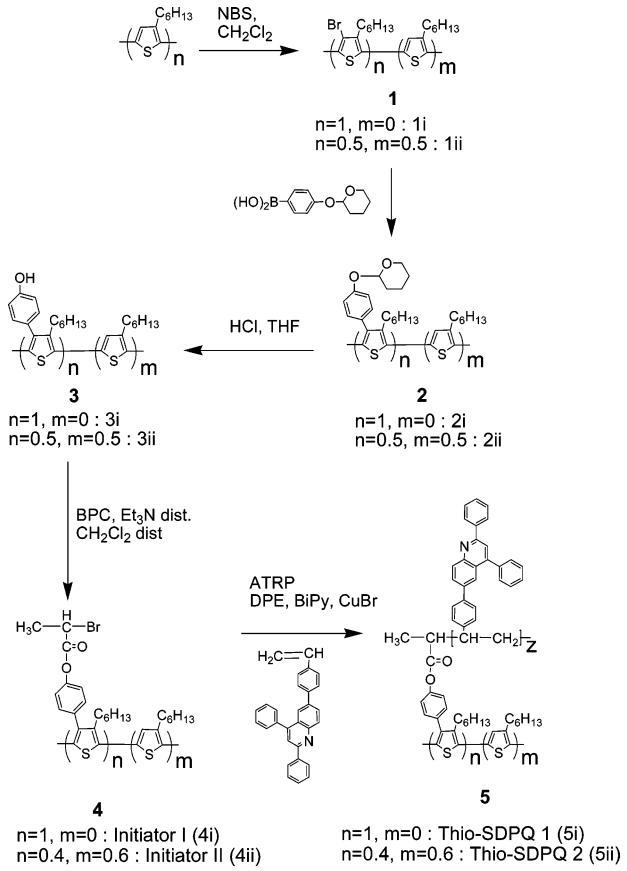


**Synthesis of 3i, 3ii.** Into a carefully degassed three-necked flask were added 270 mg of either **1i** or **1ii**, an excess of 2-tetrahydropyranyloxy-4-phenylboronic acid (350 mg, 1.57mmol), 2.4 mL of $Na_2CO_3$ 2 M, 60 mg (0.052 mmol) of $Pd(PPh_3)_4$, and 20 mL of THF. The mixture was stirred at 100 °C for 2 d, cooled down at room temperature, and precipitated into MeOH. The product was filtered and the dried powder (**2i**, **2ii**) was diluted in THF and 0.3 mL of HCl acid 37% were added, alongside, in a round flask and stirred for 1 d. The mixture was precipitated in $H_2O$, filtered, washed with $H_2O$, and dried. The polymer was dissolved in $CHCl_3$, precipitated into a 10-fold excess of MeOH, filtered, and dried, yielding **3i** (280 mg), **3ii** (250 mg).

**3i**. $^1$H-NMR ($CDCl_3$): $\delta$ 7.15−7.25 (broad, 4H), 4.82 (s 1H), 2.81 (broad, 2H), 1.56 (d, 2H), 1.28−1.33 (m, 6H), 0.91 (d, 3H).

**3ii**. $^1$H-NMR ($CDCl_3$): $\delta$ 6.99−7.12 (d, 4H) 6.81 (m, 1H), 4.86 (s, 1H), 2.81 (b, 2H), 2.7 (b, 2H), $\delta$ 1.56 (d, 4H) $\delta$ 1.28−1.33 (m, 12H) $\delta$ 0.91 (d, 6H).

**Synthesis of Macroinitiator 4i and 4ii.** In a carefully degassed round flask was added 240 mg of **3i** or **3ii** and dissolved in 60 mL of distilled $CH_2Cl_2$. The polymer solution was cooled to 0 °C. Bromopropionyl chloride (BPC), 1 mL, and 1 mL of distilled $Et_3N$ were added into the reaction, and after 10 min, the mixture was heated at 60 °C for 1 d. Then the mixture was cooled to 0 °C and 1 mL of BPC and 1 mL of distilled $Et_3N$ were added. After 10 min the mixture was heated at 60 °C for 1 d. This procedure was repeated once more, and the final mixture was left to react at 60 °C for 2 d. Finally an excess of MeOH was added to the flask, and the mixture was stirred for 1 h. The mixture was filtered, and the resulting initiator was washed with MeOH repeatedly and subsequently dried, affording **4i** (260) and **4ii** (250 mg).

**4i**. $^1$H-NMR ($CDCl_3$): $\delta$ 7.15−7.25 (broad, 4H), 4.58 (s, 1H), 2.57 (broad, 2H), 1.94 (s, 3H), 1.11−1.45 (m, 8H), 0.88 (d, 3H).

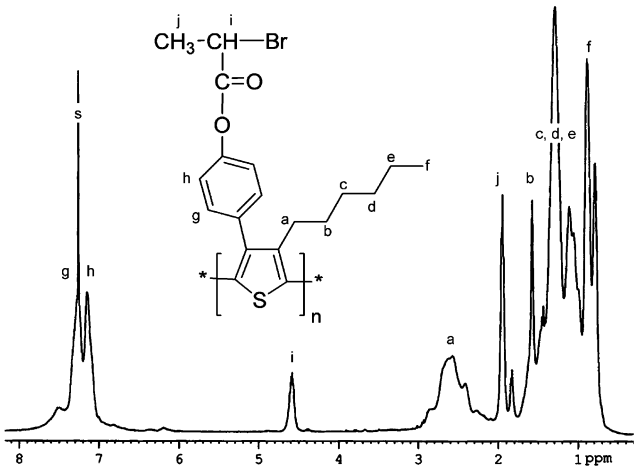

**Figure 1.** $^1$H-NMR characterization of Initiator **4i**.

**4ii**. $^1$H-NMR ($CDCl_3$): $\delta$ 7.06−7.21 (b, 4H), 6.74−6.91 (m, 1H), 4.53 (s, 1H), 2.59 (b, 2H), 2,31 (b, 2H), 1.75 (s, 3H), 1.08−1.36 (m, 16H), 0.82−0.95 (d, 6H).

**Polymer Syntheses 5i and 5ii.** A round-bottomed flask equipped with a U-tube, a rubber septum, magnetic stirrer, and a gas inlet/outlet was carefully degassed. Initiator **4i** (16 mg, 0.04 mmol) or initiator **4ii** (17 mg, 0.06mmol), was added to the flask containing CuBr (13 mg, 0.078 mmol) and 2,2′-bipyridine (12 mg, 0.078mmol) along with 2,4-diphenyl-6-(4-vinylphenyl)quinoline (150 mg, 0.39 mmol) and diphenyl ether (1.5 mL). The system was degassed three times and filled with argon. The reaction mixture was then heated at 110 °C for 24 h. After cooling, 5 mL of $CHCl_3$ was added, and the solution was filtrated through a silica column, and precipitated into an excess of MeOH. The obtained polymer was dried under vacuum.

**5i (Yield: 60 mg).** $^1$H NMR ($CDCl_3$): $\delta$ 6.50−8.19 (three broad, 22H), 1.25−2.16 (three broad, 14H), 0.83 (broad, 3H).

**5ii (Yield: 85 mg).** $^1$H NMR ($CDCl_3$): $\delta$ 7.26−8.12 (three broad, 23H), 2.36 (broad, 4H), 1.26−1.59 (two broad, 22H), 0.88 (broad, 6H).

## Results and Discussion

**Copolymer Synthesis.** The recent developments in using controlled radical polymerization techniques[23] for the realization of new polymeric architectures enable the design and synthesis of new copolymers combining blocks with different functions.[21,24] In such cases, the preparation of a macroinitiator segment which possesses a desired function is required for the development of a second segment via polymerization of the proper vinylic monomer. In accordance to this line of reasoning, we have modified commercially available polythiophene by introducing the bromine functionality to a certain extent. Using the Suzuki coupling with THP protected phenylboronic acid, subsequent deprotection and finally, esterification of the free phenol with 2-bromopropionyl chloride we end up with the desired macroinitiators **I** and **II** (Scheme 1), the first containing one propionyl bromide group in each thiophene repeating unit, (**4i**, 100%) and the second having approximately half the number of initiators (**4ii** 40%).

By employing ATRP conditions, we succeeded in the polymerization of a vinyl quinoline monomer. Two copolymers with different grafting densities were synthesized (**5i** and **5ii**). The used macroinitiators, as well as the synthesized graft copolymers, were characterized using $^1$H NMR. From the spectrum of initiator **4i** (Figure 1) we can clearly see the aromatic protons denoting the phenyl group, as well as the 4.5 ppm peak assigned to the methinic proton of the initiator. The aromatic proton attached to the thiophene ring (appearing in the spectrum at 6.95 ppm) is absent, confirming the fully substituted character of the polythiophene derivative.

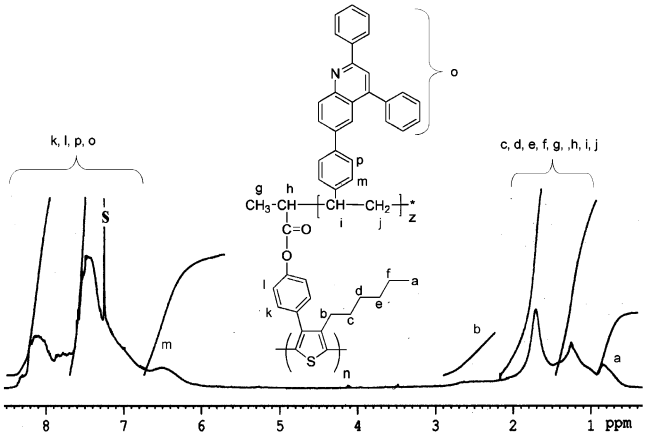

**Figure 2.** $^1$H-NMR characterization of copolymer **5i**.

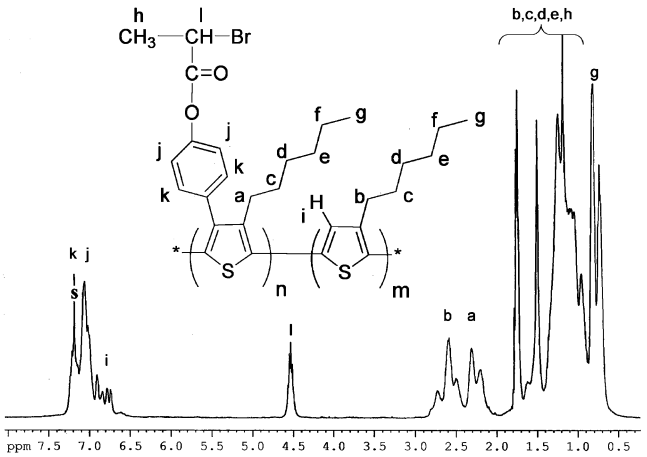

**Figure 3.** $^1$H-NMR characterization of Initiator **4ii**.

$^1$H NMR of initiator **4ii** (Figure 3) shows some differences (compared to **4i**), most notably, the split of the α-methylene protons of the hexyl side chain attached to the thiophene ring. NMR characterization can reveal the degree of functionalization which can be obtained by the comparison of the peaks at 2.3 and 2.6 ppm attributed to the α-methylene protons of the hexyl chain to the peak at 4.5 ppm of the methinic proton. Holdcroft and co-workers, in a study of various synthesized 3,4-disubstituted thiophenes[25] suggested that when a phenyl ring is attached to the 3-position of an alkyl-substituted thiophene, the α-methylene peak shifts from 2.70 to 2.26 ppm. Thus, multiple peaks appearing in the region of 2.2−2.8 ppm, could be attributed to the introduction of the aromatic rings in the initiator. NMR analysis shows that not all the bromine atoms ended up as functional initiator sites in the polymer backbone. By comparing the peak at 4.5 ppm to the peaks at 2.3 and 2.6, we conclude that the total yield of the functionalization process is approximately 75%. Roughly four out of five bromine atoms ended up as functional ATRP initiator sites. The total amount of functionalization of the initiator **II** is 40%. Finally, the multiple peaks at 6.7−6.9 ppm attributed to the aromatic proton of the thiophene moieties are worth mentioning, confirming the fact that a percentage of thiophene moieties have not been substituted.

NMR comparison, of the initiator **4i** (Figure 1) and the resulting copolymer **5i** (Figure 2) shows that the peak at 4.5 ppm attributed to the methinic protons of the initiator, has completely disappeared in the copolymer's spectrum, thus

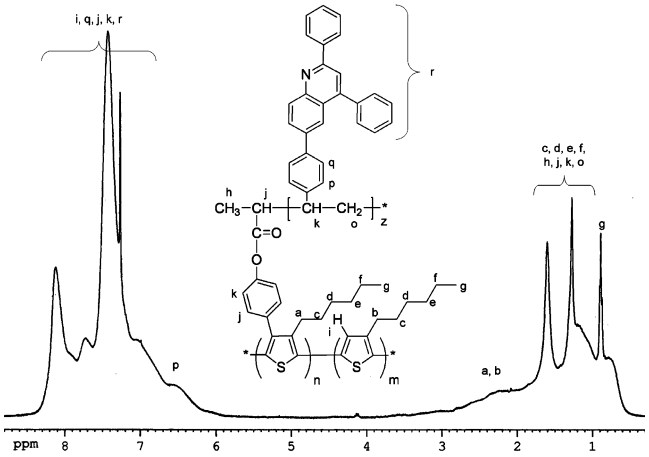


**Figure 4.** $^1$H-NMR characterization of copolymer **5ii**.

confirming the successful polymerization of the quinoline monomer. The NMR spectra of both copolymer **5i** and **5ii** (Figure 4) is dominated by the peaks attributed to the quinoline that overlap with the thiophene peaks, except from the peak at 0.83 ppm which corresponds to the methylene group of the hexyl side chain of the thiophene. Using this ratio, we can calculate the degree of polymerization of the quinoline along the thiophene backbone. In the case of copolymer **5i**, we can compare the three protons of the methyl group to all the aromatic protons. The NMR analysis shows that approximately two quinoline monomers are polymerized in every thiophene unit.

Similarly to the copolymer **5i**, we can calculate the degree of polymerization of copolymer **5ii**. The difference is that in this case, the aliphatic protons at 0.9 ppm correspond to both the substituted and the unsubstituted thiophene rings. Calculations yielded that, approximately five to six quinoline units are polymerized in every functional thiophene group.

**Optical Characterization.** The copolymers as well as the initiators were studied by UV−vis and photoluminescence spectroscopies. All the optical data are summarized in Table 1. From the optical data of the initiators, it is shown that the percentage of functionalization has an effect on the optical properties of the polythiophene. The greater the percentage, the more the optical spectra are blue-shifted. In the absorption spectra two peaks can be seen, one at 255 nm common for both initiators which is attributed to the phenylene side chain ring and one attributed to the thiophene chromophore. In the case of the fully substituted initiator (**4i**) this peak appears at 356 nm, while in the case of the partially substituted initiator (**4ii**) the peak is red-shifted to 404 nm. The effect of the side chain phenylene ring, when the polymer has a higher or lower degree of substitution is much more pronounced in the emission spectra. Both spectra are characterized by a single peak similar in shape. The photoluminescence spectra of initiator **4i** displays a peak at 506 nm while that of initiator **4ii** is red-shifted by almost 40 nm, exhibiting a peak at 540 nm. As expected, the introduction of the bulky phenyl ring in the 3-position of P3HT, disturbs the planarity of the thiophene ring, resulting in a reduction of the effective conjugated length, which is expressed as a blue shift of the photoluminescence peaks.

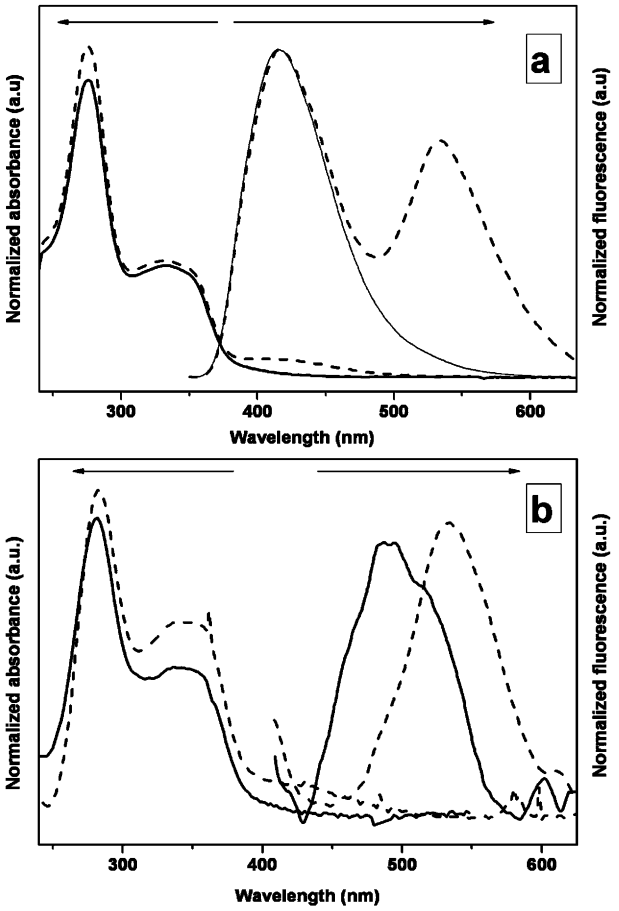


**Figure 5.** UV−vis and photoluminescence spectra of copolymer **5i** (solid line) and **5ii** (dashed line) in (a) $10^{-5}$ M $CHCl_3$ solution and (b) in thin film form.

Moving on to the copolymers **5i** and **5ii**, similar interesting observations can be seen regarding the brush-type polymer. The absorption and emission spectra in solution (Figure 5a) for the higher substituted copolymer **5i**, show the characteristics of a SDPQ homopolymer with two peaks at 276 and 335 nm attributed to the phenylene and quinoline groups respectively. It is interesting to note the complete absence of the thiophene optical absorption in the resulting copolymer. The emission spectrum follows the same pattern as only the quinoline emission is observed at 416 nm. Upon examining the UV−vis spectrum of the partly substituted copolymer **5ii**, the thiophene character can be observed by an additional shoulder at 415 nm albeit weak in intensity. The emission spectrum is much more conclusive, confirming indeed the optical presence of the thiophene backbone by a strong peak at 534 nm, similar to the 540 nm peak of the initiator **4ii**, in addition to the peak at 416 nm.

Examining the copolymers in the solid state, (Figure 5b) two peaks, characteristic of the quinoline homopolymer can be observed in the UV−vis spectra at 283 and 347 nm. In the case of copolymer **5ii** an additional weak shoulder at around 428 nm can be seen, attributed to the thiophene. The emission spectra of copolymers **5i** and **5ii**, when excited at 347 nm, display a peak at 491 in the case of copolymer **5i** and 534 nm for the **5ii**

**Table 1. Optical Data for the Synthesized Copolymers and the Modified Initiators**

| | initiator **4i** | initiator **4ii** | copolymer **5i** | copolymer **5ii** |
|---|---|---|---|---|
| UV-vis absorbance (nm) solution | 255, 356 | 255, 404 | 276, 335 | 276, 335, 415 |
| PL emission (nm) solution | 506 | 540 | 416 | 416, 534 |
| UV-vis absorbance (nm) film | 280, 350 | 276, 400 | 283, 347 | 283, 347, 428 |
| PL emission (nm) film | 497 | 537 | 491 | 534 |

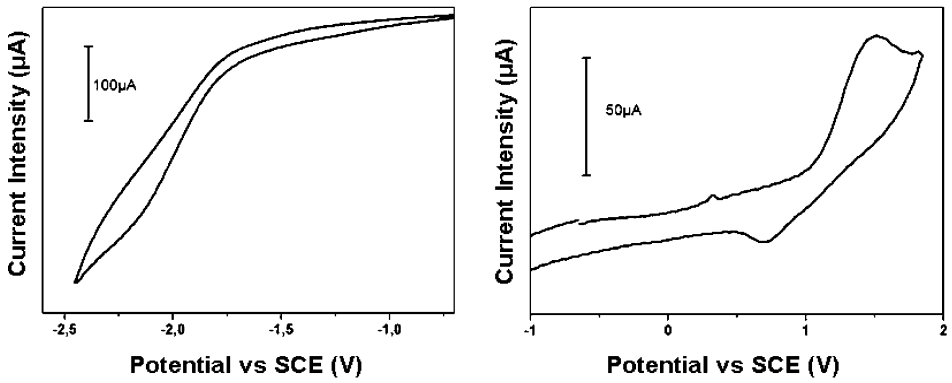


**Figure 6.** Cyclic voltammogram of copolymer **5i** in thin film cast from $CHCl_3$. Scan rate 200 mV/s. The reduction run is depicted in the left image, while the oxidation run is displayed in the right image.

copolymer. It is interesting to point out, that for the copolymer **5ii** no red shift is observed when moving from the solution to solid state. In the case of the copolymer **5i** red shift (from 416 to 491 nm) is observed when comparing emissions from solution and thin film. The peak at 491 nm must be attributed to the thiophene moiety, a peak not visible, in solution where the 416 nm emission characteristic of the quinoline can only be observed. It appears that the brush type structure of **5i** prevents the emission of the thiophene in solution.

In the case of copolymer **5ii**, the solid-state emission spectrum exhibits solely the polythiophene peak at 534 nm and not the peak attributed to the quinoline moiety (416 nm). Upon examination of the optical data in solution, the thiophene moiety's absorption at 415 nm "overlaps" with the quinoline moiety's emission at 416 nm. Thus, in solution, emission from the quinoline moieties is the predominant effect, while in the solid state; energy transfer from the quinoline blocks, to the polythiophene backbone takes place.

**Electrochemical Study.** Both copolymers were examined using cyclic voltammetry, in an effort to reveal their HOMO and LUMO energy levels. The copolymers were studied in thin film form.

In Figure 6, the cyclic voltammogram of the fully substituted copolymer **5i** is depicted. A clear oxidation at 1.50 V, which is possibly partly reversible with a reduction appearing at 0.72 V is seen. The $E_{1/2}$ of these processes yields a HOMO level of 5.5 eV. The onset of the oxidation process is located around 1.08 V, yielding, approximately, the same ionization potential, enhancing the assumption that the reduction process at 0.72 V is the dedoping process of the oxidation at 1.50 V. The reduction run yields a shoulder, peaking at around −2.05 V with an onset at −1.91 V placing the electron affinity energy level of the copolymer **5i** at 2.5 eV and the electrochemical band gap at 3.0 eV in fairly good agreement with the 3.1 eV band gap that can be calculated from the optical spectra.

Examining the voltamogram of copolymer **5ii** (Figure 7), an irreversible oxidation process is seen at 1.35 V with an onset at 1.03 V yielding an ionization potential of 5.4 eV. The reduction area of the copolymer displays a reversible n-doping/dedoping process with peaks at −1.95 and −1.80 V, respectively. The electron affinity for this polymer is estimated at 2.5 eV. When the scan rate is lowered (inset of Figure 7) the dedoping process can be seen more clearly. The electrochemical band gap remains at 2.9 eV as expected since both copolymers have similar absorption spectra.

From the electrochemical study of the two copolymers, some interesting remarks can be made. First of all, a single oxidation and reduction process was revealed, suggesting that the new

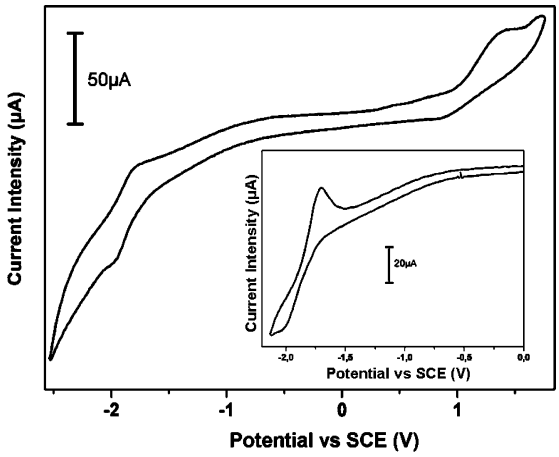


**Figure 7.** Cyclic voltammogram of copolymer **5ii** in thin film cast from $CHCl_3$. Scan rate 100 mV/s. An enlargement of the reduction run at a scan rate of 20 mV/s is shown in the inset.

brush type copolymer does not merely have the properties of the two polymers that constitute it. At first glance it appears that both copolymers are dominated by the quinoline moiety, since both their absorption and electrochemical data (HOMO−LUMO) coincide with those exhibited by the quinoline homopolymer.[21] However, the partly reversibile p-doping process that was observed for the copolymer **5i** is worth noting. Such a feature was not observed for the SDPQ homopolymer. The thiophene moiety should be responsible for the dedoping peak at 0.72 V since thiophenes are excellent electron donating materials.

On the other hand the copolymer **5ii** displays a reversible n-doping/dedoping process which is something that, also, was not observed in the SDPQ homopolymer, but rather was only seen when the SDPQ monomer was examined. The n-doping/dedoping processes suggest that copolymer **5ii** could be used as an electron acceptor.

**Compatibilization of Polythiophene/Polyquinoline Blends. A Morphological Study.** The copolymers synthesized were examined regarding the morphological properties as compatibilizers in a binary blend with P3HT and SDPQ polymers.

The primary expectation of these copolymers was to improve the morphology of the P3HT-SDPQ blend (Figure 9a). There are two main objectives for a morphological optimization on a polymer blend which will be used in an active layer in an optoelectronic application such as a photovoltaic cell. The first is to achieve a uniform morphology throughout the active layer that provides phase separation in a scale of about 10 nm which corresponds to the exciton diffusion length. The other is to reduce the roughness of the active layer.

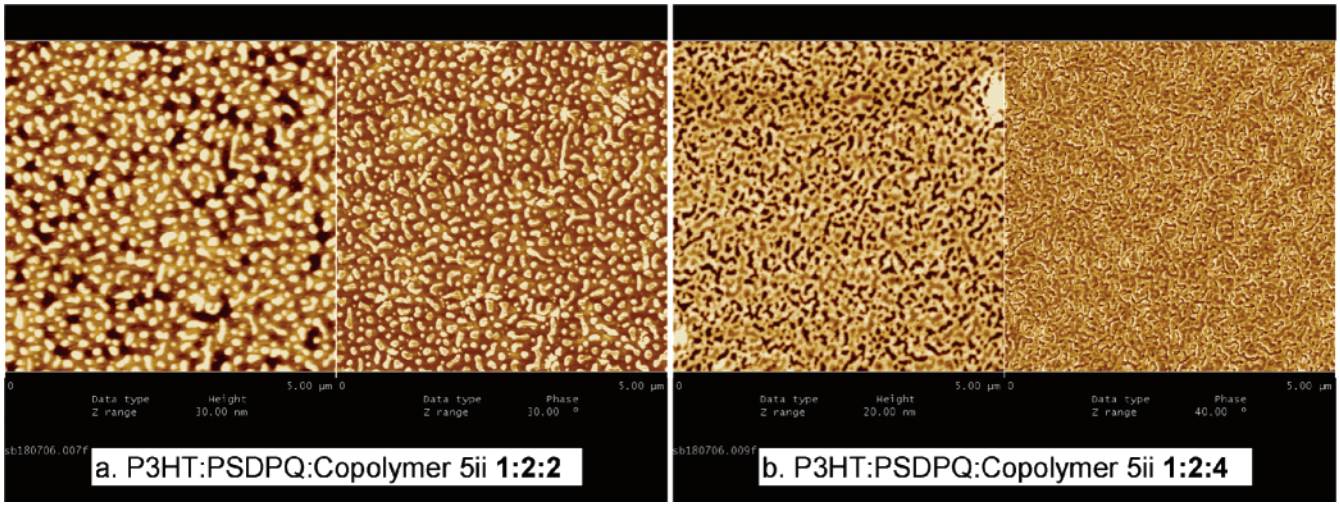


**Figure 8.** Phase topography (right pictures) and height topography (left pictures) AFM images (5 × 5 $\mu$m) of the ternary blends of a) P3HT:PSDPQ:copolymer **5ii** 1:2:2 and (b) P3HT:PSDPQ:copolymer **5ii** 1:2:4.

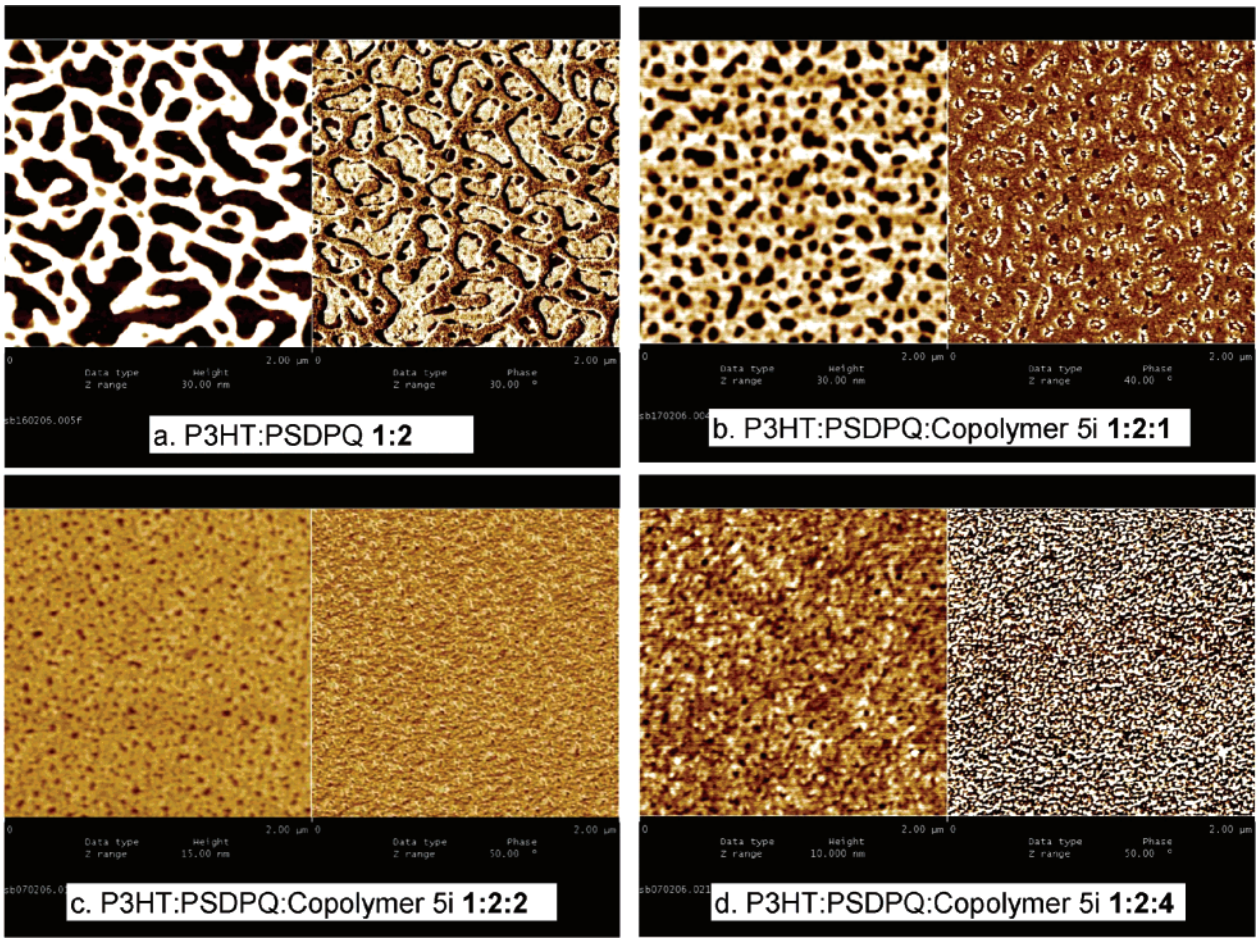


**Figure 9.** Effect of copolymer's percentage on the morphology. Phase topography (right pictures) and height topography (left pictures) AFM images (2 × 2 $\mu m$) of a) P3HT:PSDPQ 1:2 blend, (b) P3HT:PSDPQ:copolymer **5i** 1:2:1, (c) P3HT:PSDPQ:copolymer **5i** 1:2:2, and (d) P3HT:PSDPQ:copolymer **5i** 1:2:4.

Having examined the binary blends of regioregular thiophene and quinoline polymers,[26] and through the use of a selective solvent for the SDPQ polymer, we concluded through SEM and AFM techniques that in these binary blends, regardless of the ratio of the two polymers, the thiophene polymer always forms a polymeric matrix in which quinoline-rich regions can be observed. Studying various concentrations, it was deducted that some level of control in the morphology of the blend was possible through altering the composition ratio in the blend. By altering the P3HT concentration, we could achieve quinoline-rich regions in a completely phase separated blend, that extended from 40 to 50 nm in diameter, in the P3HT-rich blend, to 300 to 400 nm in the SDPQ-rich blend. Once a compatibilizing agent, such as a copolymer, is introduced in an immiscible binary blend the copolymer's architecture plays the critical role in the compatibilization efficiency. Brush copolymers tend to have a less profound compatibilizing effect than, e.g., diblock or triblock copolymers. This proves especially true in the case

of densely grafted copolymers. The side branches prevent the polymeric backbone from having an active role in the polymer−polymer interface. Should the copolymer's introduction, successfully, induce an alteration in morphology, a finer separated blend is expected, compared to the original binary blend. Moreover, in densely grafted copolymers, interesting morphologies have been observed by Moeller et al.[27] where the long side branches induce a rodlike structure for the polymeric backbone. In our case, the quinoline side chain length, was kept to a minimum, primarily, in order to enhance its compatibilizing properties, and second, to sustain the thiophene character of the resulting copolymer.

Ternary blends of P3HT:PSDPQ:copolymer **5ii** (Figure 8) reveal a completely different morphology than the binary P3HT:SDPQ blend bearing the same composition ratio of the p-type and n-type polymers (Figure 9a). Small regions in a polymer matrix are formed upon addition of copolymer **5ii** in the blend (Figure 8a). The majority of these regions is approximately 170 nm in size, but a large number of smaller various-sized "islands" are clearly observed. Increasing the amount of the copolymer **5ii** (Figure 8b) induces a different morphology. The roughness of the surface is down to 20 nm (compared to 30 nm in the 1:2:2 blend) and the surface of the thin film resembles an interpenetrating network. Rather than clear, phase separated regions, small pathways are formed, verifying the effective compatibilizing properties of the copolymer.

In Figure 9, we can see how different concentration of copolymer **5i** can alter the morphology of a P3HT−SDPQ:1−2 blend. In Figure 9a, the quinoline-rich regions appear as the larger dark areas (left picture). By introducing the copolymer **5i** in a 1:2 binary blend, we observe a great alteration in the morphology. The phase separation is now taking place in a much smaller scale. Regions of about 50−130 nm in diameter are visible. The relationship between the two morphologies is clearly discernible. The large regions in Figure 9a have been reduced in size by the addition of copolymer **5i**. Moving on to a 1:2:2 concentration, a much more homogeneous morphology is observed. Along with the further reduction of the phase separated region to an even smaller scale the addition of a larger copolymer concentration, brings about a reduction in roughness by about 30−50 nm. The *z*-axis height of parts a and b of Figure 9 is measured at 30 nm while the height in Figure 9c is about 15 nm. Finally by further increasing the copolymer's concentration to 1:2:4, we see that the morphology is again improved. Phase separation extends to 15-30 nm and roughness remains at a very good level, at 10 nm.

The clear morphological pattern that emerges from these blends is that the introduction of copolymer undoubtedly induces a smoother morphology. The phase separation is reduced by an order of magnitude and roughness is also improved.

## Conclusion

We have successfully synthesized graft copolymers bearing quinoline side chains, along a polythiophene polymeric backbone. The polythiophene was properly modified to act as a macroinitiator for the controlled, radical polymerization of the vinyl quinoline monomer, following the "grafting from" synthetic approach. Graft copolymers with different grafting densities were prepared from their respective macroinitiators. The copolymers were studied with respect to their optical and electrochemical properties. Energy transfer from the quinoline moieties to the polythiophene backbone is suggested. Atomic force microscopy was employed to examine the compatibilizing effect of the synthesized copolymers in a P3HT:PSDPQ immiscible polymer blend. Morphological studies reveal a vast improvement of the morphology with the use of the compatibilizing copolymers. Phase separation is greatly reduced, along with the roughness of the thin films, proving the successful compatibilization of the polymeric blends.

**Acknowledgment.** Financial support for this project from the Greek Ministry of Development under the research grant EPAN E13 is gratefully acknowledged.

## References and Notes

(1) Sariciftci, N. S.; Smilowitz, L.; Heeger, A. J. Wudl, F. *Science* **1992**, *258*, 1474.
(2) Yu, G.; Gao, J.; Hummelen, J. C.; Wudl, F.; Heeger, A. J. *Science* **1995**, *270*, 1789.
(3) Yu, G.; Heeger, A. J. *J. Appl. Phys.* **1995**, *78*, 4510.
(4) Hou, J.; Tan, Z.; Yan, Y.; He, Y.; Yang, C.; Li, Y. *J. Am. Chem. Soc.* **2006**, *128*, 4911.
(5) Ma, W.; Yang, C.; Gong, X.; Lee, K.; Heeger, A. J. *Adv. Funct. Mater.* **2005**, *15*, 1617.
(6) Alam, M. M.; Jenekhe, S. A. *J. Phys. Chem. B* **2001**, *105*, 2479.
(7) Kim, Y.; Cook, S.; Choulis, S. A.; Nelson, J.; Durrant, J. R.; Bradley, D. D. C. *Chem. Mater.* **2004**, *16*, 4812.
(8) (a) Arias, A. C.; MacKenzie, J. D.; Stevenson, R.; Halls, J. J. M.; Inbasekaran, M.; Woo, E. P.; Richards, D.; Friend, R. H. *Macromolecules* **2001**, *34*, 6005. (b) Alam, M. M.; Tonzola, C. J.; Jenekhe, S. A. *Macromolecules* **2003**, *36*, 6577.
(9) Alam, M. M.; Jenekhe, S. A. *Chem. Mater.* **2004**, *16*, 4647.
(10) Wu, W. C.; Liu, C. L.; Chen, W. C. *Polymer* **2006**, *47*, 527.
(11) Gebeyehu, D.; Brabec, C. J.; Padinger, F.; Fromherz, T.; Hummelen, J. C.; Badt, D.; Schindler, H.; Sariciftci, N. S. *Synth. Met.* **2001**, *118*, 1.
(12) Kim, K. A.; Park, S. Y.; Kim, Y. J.; Kim, N.; Hong, S. I.; Sasabe, H. *J. Appl. Polym. Sci.* **1992**, *46*, 1.
(13) Ramos, A. M.; Rispens, M. T.; van Duren, K. J. K.; Hummelen, J. C.; Janssen, R. A. J. *J. Am. Chem. Soc.* **2001**, *123*, 1931.
(14) Zhang, F.; Svensson, M.; Andersson, M. R.; Maggini, M.; Bucella, S.; Menna, E.; Inganäs, O. *Adv. Mater.* **2001**, *13*, 1871.
(15) Ball, Z. T.; Sivula, K.; Fréchet, J. M. J. *Macromolecules* **2006**, *39*, 70.
(16) van der Veen, M. H.; de Boer, B.; Stalmach, U.; van de Wetering, K. I.; Hadziioannou, G. *Macromolecules* **2004**, *37*, 3673.
(17) Sivula, K.; Ball, Z. T.; Watanabe, N.; Fréchet, J. M. J. *Adv. Mater.* **2006**, *18*, 206.
(18) Hoppe, H.; Egbe, D. A. M.; Mühlbacher, D.; Koppe, M.; Sariciftci, N. S. *Mol. Cryst. Liq. Cryst.* **2005**, *426*, 255.
(19) Camaioni, N.; Catellani, M.; Luzzati, S.; Migliori, A. *Thin Solid Films* **2002**, *403*−*404*, 489.
(20) Li, Y.; Vamvounis, G.; Holdcroft, S. *Macromolecules* **2001**, *34*, 141.
(21) Economopoulos, S.; Andreopoulou, A.; Gregoriou, V.; Kallitsis, J. *Chem. Mater.* **2005**, *17*, 1063.
(22) Agrawal, A. K.; Jenekhe, S. A. *Chem. Mater.* **1996**, *8*, 579.
(23) (a) Xia, J.; Matyjaszewski, K. *Chem. Rev.* **2001**, *101*, 2921. (b) Kamigaito, M.; Ando, T.; Sawamoto, M. *Chem. Rev.* **2001**, *101*, 3689.
(24) (a) Tsolakis, P. K.; Kallitsis, J. K. *Chem.*−*Eur. J.* **2003**, *9*, 936. (b) Chochos, C. L.; Tsolakis, P. K.; Gregoriou, V. G.; Kallitsis, J. K. *Macromolecules* **2004**, *37*, 2502. (c) Yu, X.-F.; Lu, S.; Ye, C.; Li, T.; Liu, T.; Liu, S.; Fan, Q.; Chen, E.-Q.; Huang, W. *Macromolecules* **2006**, *39*, 1364.
(25) Li, Y.; Vamvounis, G.; Yu, J.; Holdcroft, S. *Macromolecules* **2001**, *34*, 3130.
(26) Economopoulos, S. P.; Chochos, C. L.; Govaris, G. K.; Yiannoulis, P.; Kallitsis, J. K.; Gregoriou. V. *Mater. Res. Soc. Symp. Proc.* **2005**, *836*, L5.16.1.
(27) Beers, K. L.; Gaynor, S. G.; Matyjaszewski, K.; Sheiko, S. S.; Moeller. M. *Macromolecules* **1998**, *31*, 9413.

MA062055C